Available online at www.sciencedirect.com

SciVerse ScienceDirect

Ceramics International 38 (2012) 5501–5506

CERAMICS INTERNATIONAL

www.elsevier.com/locate/ceramint

CSA doped polyaniline/CdS organic–inorganic nanohybrid: Physical and gas sensing properties

B.T. Raut [a], M.A. Chougule [a], S.R. Nalage [a], D.S. Dalavi [b], Sawanta Mali [b], P.S. Patil [b], V.B. Patil [a,*]

[a] *Materials Research Laboratory, School of Physical Sciences, Solapur University, Solapur (MS), India*
[b] *Department o f Physics, Shivaji University, Kolhapur 416004, India*

Received 17 February 2012; received in revised form 24 March 2012; accepted 24 March 2012
Available online 1 April 2012

Abstract

Camphor sulfonic acid (CSA) doped polyaniline/CdS nanohybrid materials were prepared by chemical oxidative polymerization method and characterized by field emission scanning electron microscopy (FESEM) and Fourier transform infrared (FTIR) spectroscopy. It is proved that there is a strong synergetic interaction between the CSA and polyaniline–CdS nanohybrid. Gas sensing measurements showed that the gas sensor based on the CSA doped PANi–CdS nanohybrid had high sensor response (75%), good selectivity (for H_2S) and stability (97.34%), as well as comparatively short recovery time to H_2S, operating at room temperature. The enhanced gas sensing performance of the nanohybrid is due to the high surface area of the CSA doped PANi–CdS hybrids and the p–n heterojunction formed between p-type polyaniline and n-type CdS nanoparticles.

Keywords: CSA; PANi/CdS; Nanostructures; FESEM; H_2S sensor

1. Introduction

In recent years, conducting polymers such as polyaniline, polythiophene and polypyrrole have received much attention because of their potential applications including chemical and biological sensors, electronic devices, as well as efficient and low cost solar cells, due to their remarkable mechanical and electrical properties such as low operating temperature, low cost, flexibility and easy processability and so on [1–7]. However, there are also some disadvantages such as low chemical stability and mechanical strength that are unfavorable for conducting polymer-related applications.

Chemical sensors based on inorganic metal oxides like, WO_3, ZnO, SnO_2, Fe_2O_3, have long been studied for detecting various gases, because of their simple preparation and long-term stability [8–11]. Nevertheless, there still exist some problems with them, take ZnO for example, such as lack of selectivity, gas response and higher working temperature [12–14].

Organic–inorganic-metal oxide/conducting polymer hybrid materials are currently of great interest for exploring enhanced sensor characteristics, due to their synergetic or complementary behaviors that is not available from their single counterparts [15–17]. Much effort has been paid to investigate this kind of hybrids for gas sensor applications. Lokhande et al. [18] have synthesized the polyaniline/CdS heterostructure, which had better sensitivity than the CdS and polyaniline with respect to LPG gas exposure.

Our group has previously reported the preparation of polyaniline/CdS, polyaniline/TiO_2 and polyaniline/ZnO hybrid materials [19–21], and studied the gas sensitivity. It was found that polyaniline/CdS, Polyaniline/TiO_2 and polyaniline/ZnO hybrid materials had superior properties to their single components [22,23]. At the same time, as one kind of important conducting polymers, PANi and its derivatives have attracted considerable attention for their easy polymerization, excellent environmental and thermal stability, which is good to its application as chemical sensors [24–26].

However, with the best of our knowledge, there are no reports on the use of a CSA doped PANi–CdS nanohybrid for H_2S sensors operating at room temperature. Consequently there is a strong need for development of cost-effective sensors to

* Corresponding author.
E-mail address: drvbpatil@gmail.com (V.B. Patil).

0272-8842/$36.00
http://dx.doi.org/10.1016/j.ceramint.2012.03.064

monitor H_2S of lowest possible concentration at room temperature (300 K).

In the present work, we have prepared camphor sulfonic acid (CSA) doped an organic–inorganic nanohybrid material containing polyaniline as the organic part and CdS nanoparticles as the inorganic part by spin coating method. The gas sensors based on the hybrids were fabricated and systematically examined for gas sensing application. Obtained results showed that the hybrid materials exhibited higher sensor response, good selectivity, stability and comparatively short recovery time for detecting H_2S of a ppm level at room temperature.

2. Experimental techniques

2.1. Preparation of CSA doped polyaniline–CdS nanohybrid sensor

Camphor sulfonic acid (CSA) doped polyaniline–CdS nanohybrid sensors were prepared by adding CSA (10–50 wt%) into polyaniline–CdS nanohybrid matrix. Thin films of the CSA doped polyaniline–CdS nanohybrid were prepared on glass substrate by using spin coating technique at 3000 rpm for 40 s and dried on hot plate at 100 °C for 10 min.

2.2. Physical measurements

The morphology and chemical structure of the CSA doped polyaniline–CdS nanohybrid were carried out using Field emission scanning electron microscopy (Model: MIRA3 TESCAN operating at 20 kV) and FTIR (Model: Perkin Elmer 100 spectrophotometer). The thickness of the CSA doped polyaniline–CdS nanohybrid films was measured by using Ambios XP-1 surface profiler and it is in the range of 500–700 nm.

2.3. Gas sensing measurements

In the gas sensitivity measurements, reducing gases as C_2H_5OH, CH_3OH, NH_3, H_2S and oxidizing gases Cl_2, NO_2 were used as detecting gases. The gas sensing behaviors of CSA doped polyaniline–CdS nanohybrid were measured by custom fabricated gas sensing unit operating at room temperature. The sensing materials were deposited on glass substrate with silver electrodes, 1 mm wide and 10 mm apart from each other for the contacts. The schematic diagram of a typical gas sensor unit is shown in Fig. 1. The gas sensing measurement was in an airtight SS housing of 250 cm^3 chamber and measured quantity of desired gas (from a standard canister of 1000 ppm concentration) was injected through syringe so as to yield desired gas concentration in the housing. The electrical response of the sensor was measured with a Keithley 6514 System Electrometer, which was controlled by a computer and to measure the resistance variation of the sensor films. The definition of gas response S (%) was the ratio of $(R_a - R_g)/R_a \times 100\%$ in which R_a and R_g represented the resistance of the sensor in clear air and testing gas, respectively.

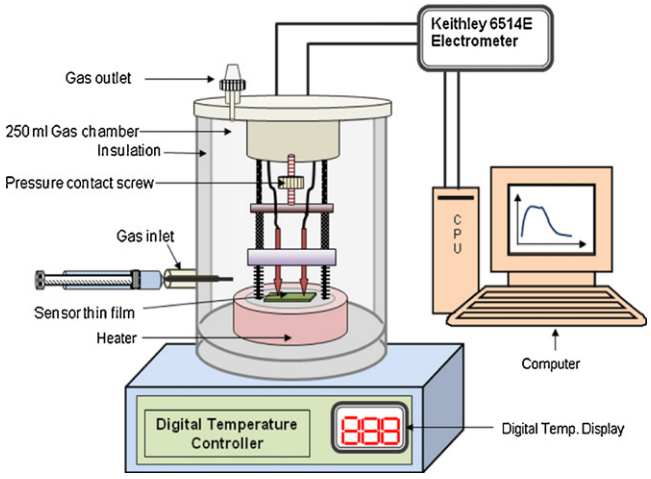

Fig. 1. Schematic of custom developed gas sensing measurement set up.

3. Results and discussion

3.1. Surface morphology analysis

The surface morphologies of PANi–CdS (50%) and PANi–CdS: CSA (10–50 wt%) are as shown in Fig. 2. In Fig. 2(a), the fibrous structure of PANi and CdS nanoparticles glued to PANi can be clearly seen [19]. The dramatic change in the surface morphology has been observed with increasing composition of CSA in PANi–CdS. At lower content of CSA (>20 wt%), the almost smooth surface is formed when the voids between the fibrous PANi–CdS is filled. With 30% of CSA, hexagonal nanopetals oriented in random direction having diameter in the range 300–600 nm are observed. At higher content of CSA (50 wt%), nanopetals are glued together.

The FESEM images helps us to draw a conclusion that the doping of CSA has a strong effect on the PANi–CdS morphology and with increase in CSA content, the composite shows a transformation in morphology from typical fibrous PANi–CdS to nanopetals.

3.2. Chemical structure analysis

The incorporation of CSA into the polyaniline–CdS nanohybrid polymer chain was confirmed by the FTIR analysis. Fig. 3 shows FTIR spectra of PANi–CdS (50 wt%) and PANi–CdS: CSA (10–50 wt%) in 500–4000 cm^{-1} wave number range. The presence of characteristic IR absorption due to quinoid and benzenoid rings at 1467 cm^{-1} and 1570 cm^{-1} clearly indicates the two states in the polymer chain. However the red shift in these two bands is observed from 1467 cm^{-1} and 1570 cm^{-1} to 1484 cm^{-1} and 1652 cm^{-1}. The broad band at 3461 cm^{-1} is due to N–H stretching of aromatic amines. The blue shift of Cd–S stretching is observed from 803 cm^{-1} to 787 cm^{-1} [19,23,27]. This red shift or blue shift can be attributed to the interaction of CSA with PANi–CdS. The presence of CSA is confirmed by the bands at 1041 cm^{-1} (SO^{3-}) and 1740 cm^{-1} (C=O) [28]. The fact that the polymer is protonated in part by surface anions is demonstrated by the

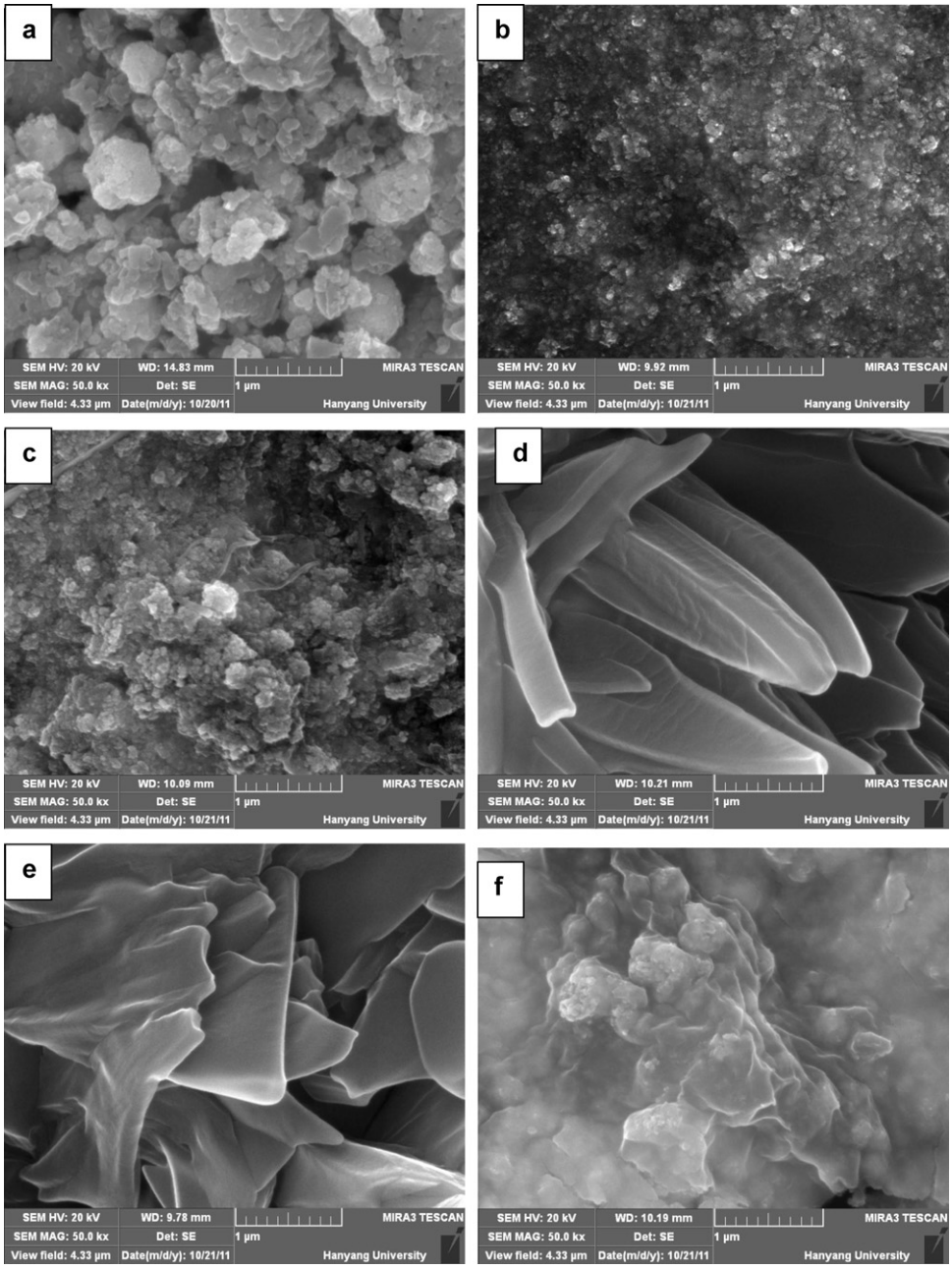

Fig. 2. FESEM of: (a) PANi–CdS (50%), (b) PANi–CdS: CSA (10%), (c) PANi–CdS: CSA (20%), (d) PANi–CdS: CSA (30%), (e) PANi–CdS: CSA (40%) and (f) PANi–CdS: CSA (50%).

presence of the peak at 588 cm^{-1}, which is attributed to a stretching vibration in the surface anion [29].

3.3. Gas sensing properties

Structural, morphological, optical and electrical studies of camphor sulfonic acid (CSA) doped PANi–CdS nanohybrid revealed that the PANi–CdS nanohybrid doped with 40 wt% of CSA showed enhanced structural, morphological and optoelectronic properties useful for gas sensing applications [30].

Therefore present study aims to study gas sensing properties of polyaniline–CdS nanohybrid doped with 40% CSA.

3.3.1. Selectivity of sensor

The ability of a sensor to respond to a certain gas in the presence of other gases is known as selectivity. Here, the selectivity measured in terms of selectivity coefficient/factor of a target gas to another gas is defined as $K = S_A/S_B$, where S_A and S_B are the responses of a sensor to a ''target gas'' A and an interference gas B, respectively.

A bar diagram of gas response of CSA (40%) doped PANi–CdS nanohybrid to H_2S, NO_2, CH_3OH, C_2H_5OH and NH_3 is represented in Fig. 4.

The PANi–CdS nanohybrid doped with 40% CSA shows higher response towards H_2S as compared to NH_3, C_2H_5OH, NO_2 and CH_3OH [($SH_2S/SNH_3 = 53.57$), ($SH_2S/SC_2H_5OH = 35.55$),

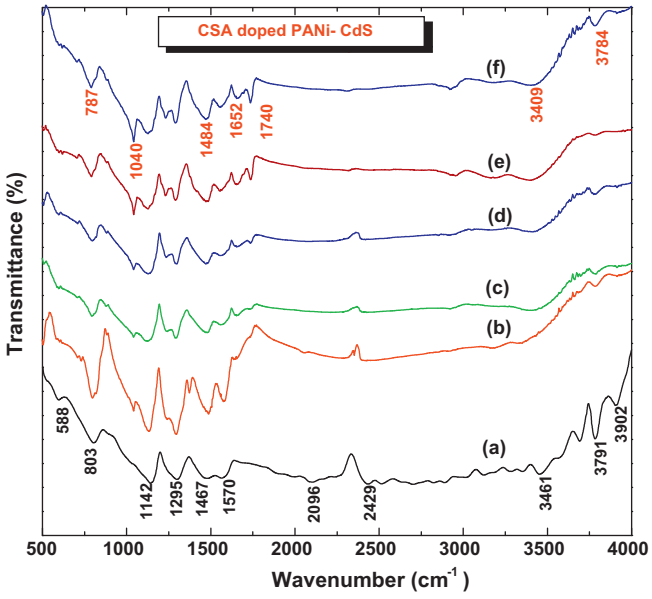

Fig. 3. FTIR spectra of: (a) PANi–CdS, (b) PANi–CdS: CSA (10%), (c) PANi–CdS: CSA (20%), (d) PANi–CdS: CSA (30%), (e) PANi–CdS: CSA (40%) and (f) PANi–CdS: CSA (50%).

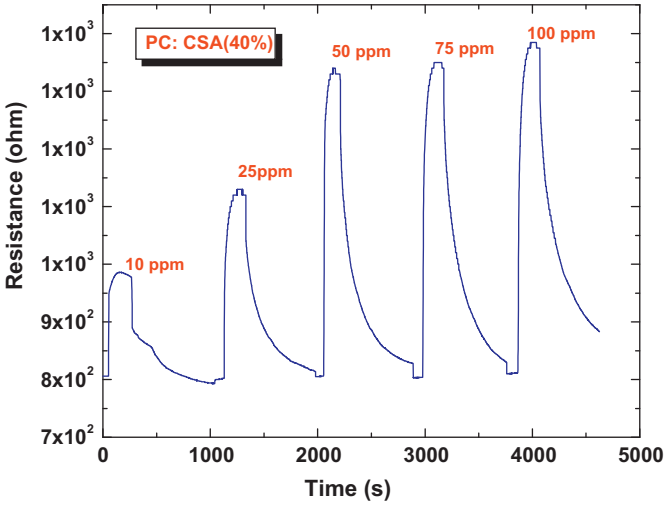

Fig. 5. Electrical response of CSA doped PANi–CdS nanohybrid sensor.

$(SH_2S/SNO_2 = 18.29)$ and $(SH_2S/SCH_3OH = 16.67)$] at room temperature. This may be due to the different gases have different energies for reaction to occur on the surface of nanohybrid. Therefore, further dependence of H_2S gas response is studied for various concentrations of H_2S at room temperature.

3.3.2. *Electrical response of CSA doped PANi–CdS nanohybrid sensor*

The initial resistance of the PANi–CdS nanohybrid thin film sensor was observed in the range of several kilo ohms [19] while the PANi–CdS nanohybrid doped with CSA showed the initial resistance of several hundreds of ohm. This enhanced conductivity can be attributed to the doping effect of CSA which maximizes the number of carriers. The highest number of carriers can be connected with the delocalized effect of doping process and formation of polarons or bipolarons in the composite structure as discussed by researchers [31,32], thus enhancing the conductivity of composite.

The resistance variation of the sensors based on PANi–CSA thin films doped with 40% CSA exposed to H_2S is as shown in Fig. 5. The concentration of H_2S was varied ranging from 10 ppm to 100 ppm. It can be seen that the resistance of CSA doped PANi–CdS nanohybrid sensor increases dramatically with time after exposed to H_2S gas, and then exponentially decreased when H_2S was replaced with air. Our sensors exhibit lower response time and higher response value but longer recovery time. This behavior may be due to higher adsorption rate than the desorption rate [31,32].

The gas response, S (%) of CSA doped PANi–CdS nanohybrid sensor at various concentrations of H_2S is shown in Fig. 6. The gas response of CSA doped PANi–CdS nanohybrid sensor was observed to increase continuously

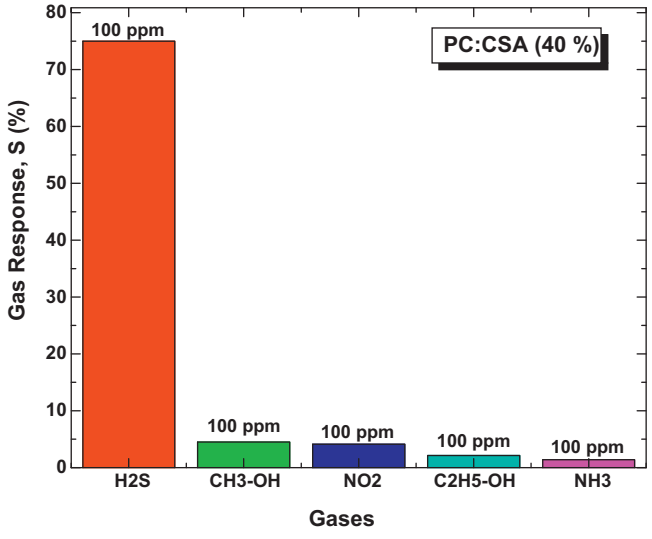

Fig. 4. Gas response of CSA doped PANi–CdS sensor to H_2S, CH_3OH, C_2H_5OH, NO_2, NH_3.

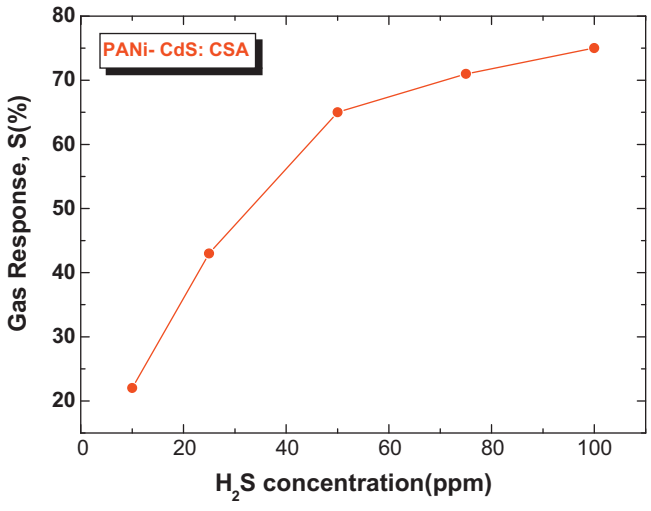

Fig. 6. Gas response of CSA doped PANi–CdS nanohybrid at various concentrations of H_2S.

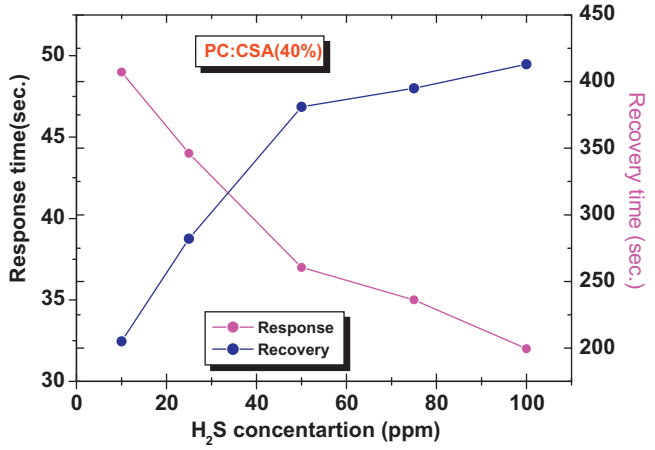

Fig. 7. Response and recovery time of CSA doped PANi–CdS nanohybrid sensor for different concentration of H_2S.

from 22 to 76% with increasing the gas concentration in the range 10–100 ppm H_2S and attains the maximum gas response. The higher gas response of CSA doped PANi–CdS nanohybrid sensor is attributed due to the porous nature of polyaniline grown on granular CdS surface which offers more chemical reactions to occur at the interface and ultimately results into increased gas response [31,32].

3.3.3. Response and recovery times of CSA doped PANi–CdS sensor

The response/recovery time is an important parameter used for characterizing a sensor. It is defined as the time required to reach 90% of the final change in current, when the gas is turned on and off, respectively. Fig. 7 shows the response and recovery times of CSA doped PANi–CdS nanohybrid sensor for different concentration of H_2S. From Fig. 7 it is observed that the response time decreased from 49 to 32 s, while the recovery time increased from 205 to 413 s as the concentration of H_2S increased from 10 to 100 ppm. This may be due to the presence of sufficient gas molecules at the surface of nanocomposite for reaction to occur. From the same graph, it is found that for higher concentrations of H_2S, the recovery time was long. This may probably be due to the heavier nature of H_2S and the reaction products are not leaving from the interface immediately after the reaction [31,32].

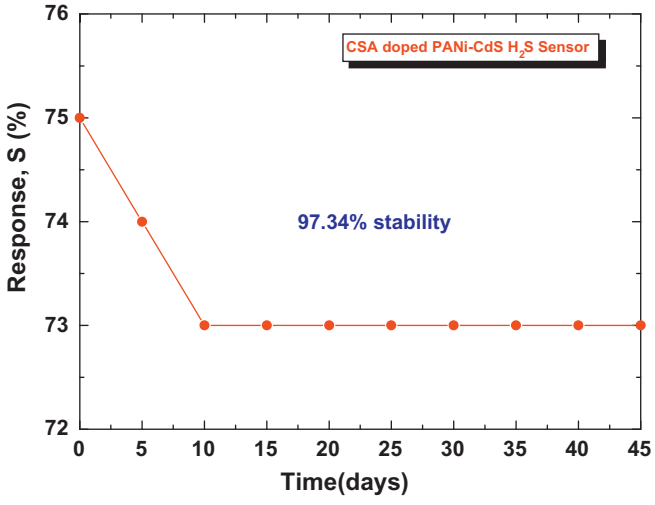

Fig. 8. Stability of CSA doped PANi–CdS nanohybrid sensor.

3.3.4. Stability and reproducibility of CSA doped PANi–CdS nanohybrid sensor

In order to check the stability and reproducibility of CSA doped PANi–CdS nanohybrid sensor, the change in resistance of nanohybrid is studied at room temperature upon exposure of fixed concentration (100 ppm) of H_2S for 45 days at an interval of 5 days, after the first measurement and the results of gas response are shown in Fig. 8. Initially CSA doped PANi–CdS nanohybrid sensor showed relatively high response, however it dropped from 75 to 73% and stable response obtained after 10 days (97.34% stability). This is because in the initial stage CSA doped PANi–CdS nanohybrid sensor may undergo interface modification during operation and then reaches to steady state indicating the stability of the CSA doped PANi–CdS nanohybrid sensor operating at room temperature.

4. Conclusions

The present work reports the preparation of CSA doped PANi–CdS nanohybrid for detection of hydrogen sulfide gas at room temperature (300 K). Morphological analysis using field emission scanning electron microscopy of the CSA doped PANi–CdS nanohybrid revealed the formation of a diffusion free surface. The gas sensing properties of nanohybrid to H_2S indicated that the thin film of CSA doped PANi–CdS nanohybrid is a candidate for H_2S detection. The maximum gas response of 76% was achieved with 97.34% stability for 40 wt% CSA doped PANi–CdS sensor upon exposure of 100 ppm H_2S working at room temperature.

Acknowledgment

Authors (VBP) are grateful to the Department of Science and Technology, New Delhi for financial support through the scheme no. SR/FTP/PS-09/2007.

References

[1] B. Adhikari, S. Majumdar, Polymers in sensor applications, Progress in Polymer Science 29 (2004) 699–766.
[2] Y.F. Zhu, S.B. Xu, L. Jiang, K.L. Pan, Y. Dan, Synthesis and characterization of Polythiophene/titanium dioxide composites, Reactive and Functional Polymers 68 (2008) 1492–1498.
[3] M. Woodson, J. Liu, Guided growth of nanoscale conducting polymer structures on surface-functionalized nanopatterns, Journal of the American Chemical Society 128 (2006) 3760–3763.
[4] B. Li, D.N. Lambeth, Chemical sensing using nanostructured polythiophene transistors, Nano Letters 8 (2008) 3563–3567.
[5] J.H. Wu, Q.H. Li, L.Q. Fan, Z. Lan, P.J. Li, J.M. Lin, S.C. Hao, High-performance polypyrrole nanoparticles counter electrode for dye-sensitized solar cells, Journal of Power Sources 181 (2008) 172–176.
[6] Q.H. Li, J.H. Wu, Q.W. Tang, Z. Lan, P.J. Li, J.M. Lin, L.Q. Fan, Application of Microporous polyaniline counter electrode for dye-sensitized solar cells, Electrochemistry Communications 10 (2008) 1299–1302.

[7] D.S. Sutar, N. Padma, D.K. Aswal, S.K. Deshpande, S.K. Gupta, J.V. Yakhmi, Preparation of nanofibrous polyaniline films and their application as ammonia gas sensor, Sensors and Actuators B 128 (2007) 286–292.
[8] D.F. Zhang, L.D. Sun, G. Xu, C.H. Yan, Size-controllable one-dimensional SnO_2 nanocrystals: synthesis, growth mechanism, and gas sensing property, Physical Chemistry Chemical Physics 8 (2006) 4874–4880.
[9] H.J. Xia, Y. Wang, F.H. Kong, S.R. Wang, B.L. Zhu, X.Z. Guo, J. Zhang, Y.M. Wang, S.H. Wu, Au-doped WO_3-based sensor for NO_2 detection at low operating temperature, Sensors and Actuators B 134 (2008) 133–139.
[10] B. Baruwati, D.K. Kumar, S.V. Manorama, Hydrothermal synthesis of highly crystalline ZnO nanoparticles: a competitive sensor for LPG and EtOH, Sensors and Actuators B 119 (2006) 676–682.
[11] Y. Wang, J.L. Cao, S.R. Wang, X.Z. Guo, J. Zhang, H.J. Xia, S.M. Zhang, S.H. Wu, Facile synthesis of porous r-Fe_2O_3 nanorods and their application in ethanol sensors, Journal of Physical Chemistry C 112 (2008) 17804–17808.
[12] G.J. Li, S. Kawi, MCM-41 modified SnO_2 gas sensors: sensitivity and selectivity properties, Sensors and Actuators B 59 (1999) 1–8.
[13] C. Bittencourt, E. Llobet, P. Ivanov, X. Correig, X. Vilanova, J. Brezmes, J. Hubalek, K. Malysz, J.J. Pireaux, J. Calderer, Influence of the doping method on the sensitivity sensors of Pt-doped screen-printed SnO_2 sensors, Sensors and Actuators B 97 (2004) 67–73.
[14] K. Chatterjee, S. Chatterjee, A. Banerjee, M. Raut, N.C. Pal, A. Sen, H.S. Maiti, The effect of palladium incorporation on methane sensitivity of antimony doped tin dioxide, Materials Chemistry and Physics 81 (2003) 33–38.
[15] D.C. Schnitzler, M.S. Meruvia, I.A. Hummelgen, A.J.G. Zarbin, Preparation and characterization of novel hybrid materials formed from (Ti,Sn)O_2 nanoparticles and polyaniline, Chemistry of Materials 15 (2003) 4658–4665.
[16] F.H. Kong, Y. Wang, J. Zhang, H.J. Xia, B.L. Zhu, Y.M. Wang, S.R. Wang, S.H. Wu, The preparation and gas sensitivity study of polythiophene/SnO_2 composites, Materials Science and Engineering B 150 (2008) 6–11.
[17] J. Zhang, S.R. Wang, M.J. Xu, Y. Wang, H.J. Xia, S.M. Zhang, X.Z. Guo, S.H. Wu, Polypyrrole-coated SnO_2 hollow spheres and their application for ammonia, sensor, Journal of Physical Chemistry C 113 (2009) 1662–1665.
[18] D.S. Dhawale, D.P. Dubal, V.S. Jamadade, R.R. Salunkhe, S.S. Joshi, C.D. Lokhande, Room temperature LPG sensor based on n-CdS/p-polyaniline heterojunction, Sensors and Actuators B 145 (2010) 205–210.
[19] B.T. Raut, P.R. Godse, S.G. Pawar, M.A. Chougule, V.B. Patil, New method for fabrication of polyaniline–CdS sensor for H_2S Gas detection, Measurements 45 (2012) 94–100.
[20] S.L. Patil, M.A. Chougule, S.G. Pawar, S. Sen, V.B. Patil, Development of Polyaniline–ZnO nanocomposite gas sensor, Sensors and Transducers Journal 34 (2011) 120–131.
[21] S.G. Pawar, S.L. Patil, M.A. Chougule, B.T. Raut, S. Sen, V.B. Patil, Room Temperature ammonia gas sensor based on Polyaniline/TiO_2 nanocomposites, IEEE Sensors Journal 11 (12) (2011) 3417–3423.
[22] S.G. Pawar, S.L. Patil, A.T. Mane, B.T. Raut, V.B. Patil, Growth, characterization and gas sensing properties of polyaniline thin films, Archives in Applied Science Research 1 (2) (2009) 109–114.
[23] B.T. Raut, P.R. Godse, S.G. Pawar, M.A. Chougule, D.K. Bandgar, S. Sen, V.B. Patil, Novel method of fabrication of CdS sensor for H_2S monitoring, Journal of Materials Science - Materials in Electronics 23 (2012) 956–963.
[24] S.S. Joshi, C.D. Lokhande, S.-H. Hanb, A room temperature liquefied petroleum gas sensor based on all-electrodeposited n-CdSe/p-polyaniline junction, Sensors and Actuators B 123 (2007) 240–245.
[25] S.G. Pawar, S.L. Patil, M.A. Chougule, B.T. Raut, S.A. Pawar, P.R. Godse, V.B. Patil, New method for Fabrication of CSA doped PANi–TiO_2 thin film ammonia sensor, IEEE Sensors Journal 11 (11) (2011) 2980–2985.
[26] S.L. Patil, M.A. Chougule, S. Sen, V.B. Patil, Measurements on room temperature gas sensing properties of CSA doped polyaniline–ZnO nanocomposites, Measurements 45 (2012) 243–249.
[27] S.S. Kawar, B.H. Pawar, Synthesis and characterization of CdS n-type of semiconductor thin films having nanometer grain size, Chalcogenide Letters 6 (2009) 219–225.
[28] E.N. Konyushenko, J. Stejkal, M. Trchova, J. Hradil, J. Kovarova, J. Prokes, M. Cieslar, J. Hwang, K. Chen, I. Sapurina, Multi-wall carbon nanotubes coated with polyaniline, Polymer 47 (2006) 5715–5723.
[29] E. Kymakis, I. Alexandou, G.A.J. Amaratunga, Single walled carbon nanotube–polymer composites: electrical, optical and structural investigations, Synthetic Metals 127 (2002) 59–62.
[30] B.T. Raut, P.R. Godse, D.K. Bandgar, M.A. Chougule, V.B. Patil, Polyaniline–CdS nanocomposites: effect of camphor sulfonic acid doping on structural, microstructural, optical and electrical properties, Journal of Materials Science - Materials in Electronics, doi:10.1007/s10854-012-0708-7, in press.
[31] H. Tai, Y. Juang, G. Xie, J. Yu, X. Chen, Z. Ying, Influence of polymerization temperature on NH_3 response of PANI/TiO_2 thin film gas sensor, Sensors and Actuators B 129 (2008) 319–326.
[32] A. Uygun, O. Turkoglu, S. Sen, E. Ersoy, A.G. Vavuz, G.G. Batir, The electrical conductivity properties of polythophene/TiO_2 nanocomposites prepared in the presence of surfactants, Current Applied Physics 9 (2009) 866–871.